

## Development of thermal regime control for crucibleless AHP method

*V.I.Deshko, V.D.Golyshev<sup>\*</sup>, A.Ya.Karvatskii, Yu.V.Lokhmanets*

National Technical University of Ukraine "Kyiv Polytechnical Institute",  
37 Pobedy Ave., 03056 Kyiv, Ukraine

<sup>\*</sup>Center for Thermal Physics Research "Thermo", 2 Gagarin St.,  
post box 2a, Aleksandrov, Vladimir Region, 601655 Russia

*Received September 25, 2007*

The results of control possibility investigation for crucibleless AHP crystal growth method are considered. Numerical studies have been carried out basing on a specially designed global heat exchange model. The control methods based on radiation flux variation are considered. The changes of diaphragm opening in a diathermic cavity under a crystal and circular gap in the lateral thermal insulation against the melt surface have been found to change substantially the temperature fields and thermal fluxes at crystallization front due to the variations of radiation fluxes to the environment. The effect of the diaphragm height location and of diaphragm and surrounding constructions thermal-physical properties on the crystallization front shape have been considered.

Рассматриваются результаты исследования возможностей управления выращиванием кристаллов бестигельным методом ОТФ. Численные исследования выполнены на базе специально разработанной модели глобального теплообмена. Рассмотрены методы управления, основанные на изменении радиационных потоков. Установлено, что при изменении степени открытости диафрагмы в диатермической области под кристаллом и зазора в боковой теплоизоляции напротив расплава существенно изменяются температурные поля и тепловые потоки на фронте кристаллизации за счет изменения радиационных потоков в окружающую среду. Проведен анализ влияния расположения диафрагмы по высоте и теплофизических характеристик диафрагмы и окружающих конструкций на положение и форму фронта.

There are numerous methods of crystal growth from melt, which are divided into three large groups according to the features of the single crystal shape formation and nucleation: 1) growth methods in ampoules; 2) growth methods by pulling from melt on seed; 3) growth methods from melt on single crystal seed using the shaping capillary elements. In this work, crystal growth by new crucibleless method, referred to as the "axial heat flux near crystallization front" (AHP) method [1], is considered. The crucibleless AHP method is based on melt holding (due to wetting forces) on the heater placed near the phase interface. The AHP method provides almost flat isotherm

and crystallization front shape over the whole crystal cross-section. The melt flow is laminar. An effective composition control is possible in AHP method which is especially important at crystallization of multi-component or doped crystals. In this method, the crystal faces are formed at large temperature gradients in the melt, and their size can occupy the whole section area of growing crystal. All these factors simplify substantially the process description and make it possible to develop quantitative models of heat and mass transfer.

The problem of crystal growth process control consists of two tasks: the control of the crystallization process itself and crystal

shaping control [2]. The crystallization process control can be carried out by different ways, for example, by moving the crystal-melt system within a varying temperature field or by temperature field variation by the heater powers control. Development of similar control methods is based on simulation of thermal processes [3]. That is why the manufacturing and processing of semi-transparent materials is closely related to the research development in the area of complex heat exchange at high temperatures. The role of radiation-conductive heat exchange for the crucible variant of AHP method is shown in [4]. In this work, another process control technique is considered based on the radiation flux control in the system of transparent and semitransparent bodies [5].

The aim of this work is to consider the control possibilities at crystal growth from melt using numerical models within a whole crystal growth setup. Unlike previous works [3], where considered were the control possibilities by the crystal-melt system moving in a varying temperature field and by temperature field variation by means of the heater powers change, this work is aimed at another variant of process control basing on the radiation flux control in the system of transparent and semitransparent bodies. To that end, a diaphragm (screen) and gaps in certain setup parts can be used. The study methods are numerical experiments.

*The problem definition.* Assume  $M$

$\Omega = \bigcup_{k=1}^M \Omega_k \in R^3$  is an area consisting of

sets  $\Omega_k$  (construction elements of the crystal growth setup), boundaries of which form a combination of piece-flat sets  $\Gamma = \Gamma_0 \cup \Gamma_4$ , at  $k = \overline{1, m}, m < M$ , solids where the heat exchange is due to heat conductivity are examined, while at  $k = \overline{m+1, M}$ , diathermic cavities where the radiation heat exchange mechanism acts. On  $\Gamma_0$ , the construction / environment boundaries and symmetries are considered, and  $\Gamma_4$  is a set of contacts between different construction elements. Because on  $\Gamma_0$  various boundary conditions (BC) are specified, let this boundary be presented as the following set:  $\Gamma_0 = \Gamma_2 \cup \Gamma_3$ , where  $\Gamma_2$  are crystallizer symmetry boundaries,  $\Gamma_3$  are an external construction boundaries with convective BC. Due to radiation heat exchange, the  $\Gamma_4$  boundary is combined:  $\Gamma_4 = \Gamma_{4T} \cup \Gamma_{4TR}$ , where  $\Gamma_{4T}$  is the

set of contacts between different heat-conducting bodies  $\Omega_k$  only,  $\Gamma_{4TR}$  is set of contact boundaries between diathermic cavities and heat-conducting elements of construction.

In terms of the above, the temperature field  $T$  in  $\Omega$  considering complex heat exchange can be described by the following system of equations (heat conduction equation and that of radiation heat exchange between opaque surfaces) with proper boundary conditions:

$$\Omega_k: \begin{cases} \text{div}[\lambda_k(T)\nabla T(X)] + q_{vk}(X) = 0, (k = \overline{1, m}); \\ \sigma T_y^4 - \int_F \sigma T_x^4 \frac{\cos\varphi_x \cos\varphi_y}{\pi|x-y|^2} \beta(x, y) dF = \\ = \frac{1}{\varepsilon_y} q_r(y) - \int_F \frac{1 - \varepsilon_x}{\varepsilon_x} q_r(x) \frac{\cos\varphi_x \cos\varphi_y}{\pi|x-y|^2} \beta(x, y) dF, \\ (k = \overline{m+1, M}), \quad x, y \in \Gamma_4 \end{cases} \quad (1)$$

symmetry conditions (adiabatic conditions):

$$\Gamma_2: \mathbf{n} \cdot \nabla T = 0; \quad (2)$$

convection heat exchange conditions:

$$\Gamma_3: \mathbf{n}[-\lambda_k(T)\nabla T] = \alpha_{eff}(T|_{\Gamma_3} - T_d); \quad (3)$$

contact heat exchange conditions:

$$\Gamma_4: \begin{cases} \Gamma_{4T}: \begin{cases} T=0; \\ \mathbf{n} \cdot \mathbf{q} = 0; \end{cases} \\ \Gamma_{4TR}: \begin{cases} T=0; \\ \mathbf{n}[-\lambda_k(T)\nabla T] = q_r, \end{cases} \end{cases}, \quad (4)$$

where  $\lambda_k(T)$  is the  $\Omega_k$  heat conductivity,  $W/(m \cdot K)$ ;  $T$ , temperature,  $K$ ;  $\nabla$ , Hamiltonian;  $X(x, y, z) \in \Omega$ , Cartesian coordinates,  $m$ ;  $q_{vk}$ , intensity of the internal heat source in  $\Omega_k$ ,  $Wt/m^3$ ;  $\sigma$ , Stefan-Boltzman constant,  $W/(m^2 \cdot K^4)$ ;  $F$ , the diathermic area surface;  $|x-y|=r$ , distance between points  $x$  and  $y$  on the  $F$  surface,  $m$ ;  $\varepsilon$ , the  $F$  surface emissivity factor;  $\varphi_x, \varphi_y$  angles between normals to surface  $F$  in points  $x, y$  and the vector  $\mathbf{r}$ , rad;  $q_r$ , radiant flux density,  $W/m^2$ ;  $T_{cr}$ , the crystallization temperature,  $K$ ;  $\Delta T$ , the smoothing interval,  $K$ ;  $\mathbf{n}$ , an external normal to boundary  $\Gamma$ ;  $\alpha_{eff}$ , effective heat transfer coefficient,  $W/(m^2 \cdot K)$ ;  $T_d$ , the environment temperature,  $K$ ;  $\{T = T^+ - T^-, T^\pm\}$ , values of function on the right and on the left of  $\Gamma_4$ ,  $K$ ;  $\{\mathbf{n} \cdot \mathbf{q}_\lambda = \mathbf{n}^+ \cdot \mathbf{q}_\lambda^+ - \mathbf{n}^- \cdot \mathbf{q}_\lambda^-\}$ ;  $\mathbf{q}_\lambda$ , vector of the conductive heat flux

density,  $W/m^2$ ;  $\mathbf{q}_\Sigma = \mathbf{q}_\lambda + \mathbf{q}_r$ , total heat flux density in diathermic medium,  $W/m^2$ ;  $\mathbf{q}_\Sigma = \mathbf{q}_r$ , total heat flux density in transparent medium,  $W/m^2$ ;  $\mathbf{q}_\Sigma = \mathbf{q}_\lambda$ , total heat flux density in non-transparent medium (heat conductivity medium),  $W/m^2$ ;  $\Omega_{ki}$ , the solid-melt joint space;  $M$ , number of areas (construction elements);  $\beta(x,y) = 1$  if point  $x$  is visible from point  $y$ , otherwise 0. The system (1) of integral-differential equations in combination with boundary conditions (2)–(4) is a complete mathematical formulation of the problem defined, representing the thermal conditions at crystal growth by AHP method in full enough. It has been taken into account that convection influence on the heat exchange conditions in melt is negligible in AHP method [6].

The global heat exchange model for crucibleless AHP method has been developed; the sizes of areas  $\Omega_k$ , corresponding to construction elements are shown in scale in Fig. 1, which gives the concept of the model geometrical dimensions. The solution method for the problem formulated is based on boundary elements method [7–9]. Unlike [10], it is assumed in the model that the heat exchange in a crystal and diathermic cavities is caused only by radiation. The model is axial-symmetric, therefore, only right part of longitudinal section is shown. A crystal is assumed to be fully transparent, with refraction index equal to 1, and non-heat-conducting. The model provides the dynamic iterative movement of the crystallization front basing on the data about crystallization temperature isotherm calculated at the previous iteration. Thus, the model allows to trace the position and form of crystallization front (under assumption that heat removal from the front is caused only by radiation).

Thermal-physical properties of materials used in the model are as follows: heat conductivity ( $W/(m \cdot K)$ ) of the melt 0.2, heaters (effective) 20, diaphragm material and tubular crystal support 79, upper rod (effective) 2, alundum tubes and disks 7, heat insulation material 1; emissivity on boundaries  $\Gamma_{4TR}$  of the melt surface 0.75, diaphragms and crystal support 0.28, alundum tubes and disks 0.5, AHP heater, insulation and upper rod 0.2. The contact between these heat-conducting elements corresponds to  $\Gamma_{4T}$  boundary conditions, and for elements adjacent to the symmetry axis, boundary conditions  $\Gamma_2$  are specified. The

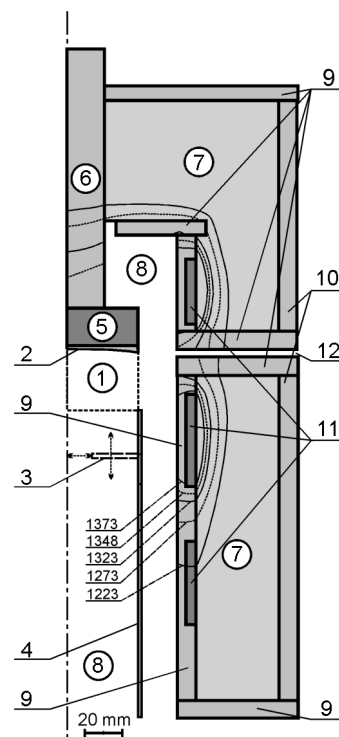


Fig. 1. General view of crucibleless AHP crystal growth setup. 1, crystal; 2, melt; 3, movable diaphragm; 4, tubular crystal support; 5, 6, AHP-heater and rod above it; 7, heat insulation; 8, diathermic cavities; 9, 10, alundum disks and tubes; 11, lateral heaters: upper, middle and lower; 12, circular gap in lateral heat insulation. 1373...1223 — corresponding isotherms (K) positions.

following convective boundary conditions were specified for alundum tubes and upper rod external surfaces: ambient temperature  $t = 50^\circ\text{C}$  (323 K), heat transfer coefficient  $\alpha = 10 \text{ W}/(\text{m}^2\text{K})$ . For the calculation of radiation heat exchange with environment, the ambient temperature is also assumed to be 323 K. The crystallizing material is characterized by properties similar to bismuth germanate  $\text{Bi}_4\text{Ge}_3\text{O}_{12}$  (BGO); thus, the crystallization temperature is assumed to be 1323 K. To verify the model adequacy, it was tested by comparing to the strict models of radiation-conductive heat transfer in semitransparent materials [11] and to models with conductive elements and effective heat conductivity [10].

*Computation results.* Several calculations series of quasi-steady-state conditions have been carried out using the developed global heat exchange model. The calculations made for the different variants of diaphragm position in height and its opening, circular gap widths in lateral heat insulation, and

also change some other geometrical and thermal-physical parameters of model. The diaphragm opening in this case is the ratio of diaphragm aperture diameter to crystal diameter:  $k = d_0/d_{cr} \cdot 100 \%$ ; at  $k = 0$ , the diaphragm is fully closed, at  $k = 100 \%$ , completely opened, i.e. absent.

As the initial model state, the diaphragm absence and the lateral heat insulation gap size of 4 mm is assumed. The diaphragm opening was varied for its height position at the level of 160 mm from the diathermic cavity bottom, that corresponds 5 mm distance from the diaphragm topside to the lower surface of "crystal" (having a height of 30 mm). In these conditions, the heater powers were selected for providing the suitable temperature fields and gradients in melt at completely opened diaphragm ( $k = 0$ ). Thus, this position was chosen as the initial one, the powers of heaters being as follows: AHP heater, 50 W; upper lateral one, 1250 W; middle lateral, 1250 W; lower lateral, 500 W. The temperature field for the initial state is shown in Fig. 1.

To estimate quantitatively the influence of the model parameters on the crystallization front position, the parametric analysis of model sensitivity has been carried out. The following influencing parameters were considered: 1) diaphragm opening; 2) diaphragm position in height (closed and partially opened,  $k = 50 \%$ ); 3) height of gap in lateral heat insulation against the melt at the opened and closed diaphragm; 4) heat conductivity  $\lambda_{tube}$  and emissivity of tubular support under the crystal at the opened and closed diaphragm; 5) power of

each heater:  $P_1, P_2, P_3$  (upper, middle and lower lateral ones, respectively) and  $P_{AHP}$  (axial). As the sensitive characteristic, the crystal thickness was chosen. The crystal thickness that defines the crystallization front position is presented by two quantities: the crystal thickness at the symmetry axis (in the center) and at its periphery (lateral surface). The sensitivity analysis consists in a sequential disturbance (change from the chosen initial position) of each parameter separately followed by numerical calculation according to the model and calculation of sensitivity value as,

$$Z_i = \frac{\Delta P}{\Delta y} \cdot \frac{y_0}{P_0}, \quad (5)$$

where  $P_0, \Delta P$  are the initial value of influencing parameter and its change;  $y_0, \Delta y$ , the initial value of crystal height and its change.

The results of sensitivity analysis are presented in Table. The strongest influence on the front position is seen to be due to changes of heater powers (the AHP heater influence looks relatively low because of low absolute value of its power), as well as to the diaphragm opening and its position. Generally, influence of most parameters appears more substantial in the peripheral (lateral) areas of the system, than in central one (close to the axis). However, it is to note that the displacement of the partly opened diaphragm influences first of all the central areas. This local influence became even more increased as the crystal height is diminished. Obviously, the effect of dia-

Table. Results of parametric sensitivity analysis

No.	Influencing parameter	Sensitivity value	
		on axis	on perimeter
1	Diaphragm openness degree — 75 % / 50 % / 25 % / 0 %	0.043 / 0.078 / 0.183 / 0.272	0.154 / 0.345 / 0.359 / 0.298
2	Position of closed diaphragm 140 / 20 mm	0.294 / -0.074	0.398 / 0.064
3	Position of 50 % opened diaphragm 140 mm / 20 mm	0.241 / 0.053	-0.094 / -0.008
4	Gap 1 mm / 6 mm at opened diaphragm	0.038 / 0.010	0.182 / 0.040
5	Gap 1 mm / 7 mm at closed diaphragm	0.245 / 0.338	0.324 / 0.583
6	$\lambda_{tube} = 5 \text{ W/(m}\cdot\text{K)} / 80 \text{ W/(m}\cdot\text{K)}$ , closed diaphragm at upper position	0.051 / 0.025	0.058 / 0.027
7	$\lambda_{tube} = 5 \text{ W/(m}\cdot\text{K)} / 80 \text{ W/(m}\cdot\text{K)}$ , closed diaphragm at lower position	0.059 / 0.031	0.076 / 0.047
8	Powers $P_1 / P_2 / P_3 / P_{AHP}$	-0.553 / -0.719/ -0.102 / -0.043	-1.513 / -1.704/ -0.229 / -0.055

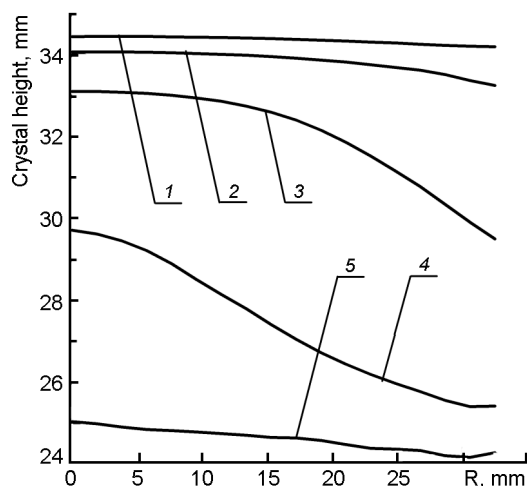


Fig. 2. Crystallization front position dependence on the diaphragm opening degree. 1 — diaphragm 100 % opened; 2 — 75 %; 3 — 50 %; 4 — 25 %; 5 — diaphragm closed.

phragm and gap change caused by radiation heat exchange has the least inertia at thermal regime control. The influence of thermal-physical properties (heat conductivity and emissivity) of tubular support is noticeable only at closed diaphragm being in lower position.

The numerical experiments have shown that as the opening of diaphragm (located in upper position 5 mm from the crystal bottom at initial height) is varied, the temperature fields and thermal fluxes at the crystallization front change very substantially due to changes in radiation fluxes to environment (downward). Comparison with the completely closed diaphragm state shows that as diaphragm is opened, the thermal flux at the crystallization front increases by several times (approximately by a factor of 4); accordingly, at constant heater powers, the melt temperature goes down sharply, resulting in crystallization and melt thickness decrease down to 1–2 mm. The most considerable changes take place in circular areas corresponding to the opening/closing diaphragm area. However, sharp state changes may occur in other areas. For example, a cooling is possible in the peripheral melt areas at partial diaphragm opening due to the circular gap influence, resulting in crystallization in this area and concave crystallization front shape. In some cases, the temperature of the AHP heater and melt may drop below the crystallization temperature and, consequently, crystallization of the whole melt layer occurs.

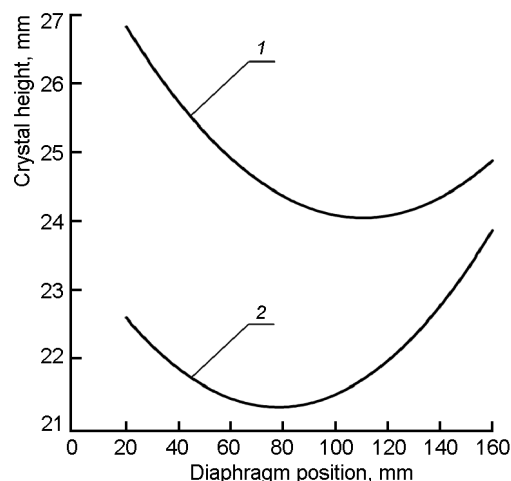


Fig. 3. Crystal height at the axis (1) and at periphery (2) dependence on closed diaphragm position in height.

Therefore, to control the crystallization process precisely, it is sufficient to change the diaphragm opening within a narrow range. The crystallization front shape and position for different opening values of diaphragm (being in upper position) are shown in Fig. 2.

As the diaphragm (fully or partially closed) is displaced in height, the temperature fields and thermal fluxes (and thus the front position) also change considerably. At initial diaphragm movement downwards approximately to the middle position, the melt thickness increases, while at further diaphragm lowering, it decreases. This effect, presented in Fig. 3 for the front position at the axis and at the periphery, can be explained by the diaphragm temperature ratio as well by that between the upper and lower parts of crystal support, along which the diaphragm moves. The upper support part, being heated by lateral heaters, has the highest temperature, and practically does not influence the crystal-melt system at upper diaphragm position, but additionally heats the system at partial diaphragm lowering. A diaphragm has a few lower temperature because it emits heat to environment (downward). In the lower diaphragm position, the coldest lower part of the support influences also crystal-melt system, resulting in melt cooling and its thickness diminution. Generally, the heater powers ratio (especially lateral middle and lower) and thermal-physical properties of diaphragm and the support (heat conductivity and reflectivity) can change considerably

the character and extent influence of the diaphragm position on the front position and shape.

The influence of the diaphragm opening was studied additionally at its closer position to crystallization front ( $h = 180$  mm), the crystal height was assumed to be of 10 mm. The distance between front and diaphragm in this case was approximately 15 mm. The supposed influence intensification of diaphragm opening on crystallization front shape and position at its approaching to the front has been confirmed. It should be noted that at diaphragm position close to the front and its partial opening, the diaphragm influence on the front is mainly local. That is, the front in its central area (corresponding to the diaphragm opened area) has a smaller thickness than in periphery area (if not consider the circular gap effect, see below), while as the diaphragm is moved off from the front, the change in its opening influences more globally on the front as a whole (see Fig. 2).

To study the circular gap width influence, a series of calculations has been carried out at its different values. The crystallization front position and shape depending on the gap width are presented in Fig. 4 for opened and closed diaphragm being in initial position. It is seen that the presence of circular gap in lateral heat insulation against the opened melt surface results in a considerable cooling of the melt peripheral area, that mostly results in concave interface shape, especially in peripheral areas. In order to avoid this effect, either the gap width decrease (this effect is insignificant at the gap less than 2 mm) or its screening (with brief opening when necessary) is needed. Thus, it is possible to control the crystallization front shape by the gap width change or its screening (at a narrow gap, the front shape is convex, at wider one, concave), and also to change the melt thickness within some limits (mainly in the peripheral area, while the diaphragm at small opening influences mainly the central melt area). Thus, change of lateral heat insulation gap width is another method of crystallization front control.

To conclude, the calculations results are obtained characterizing crystallization thermal regime control possibilities based on a radiation heat exchange for crucibleless AHP method. The diaphragm opening variation in diathermic cavity under the crystal has been found to result in considerable variations of the temperature fields and

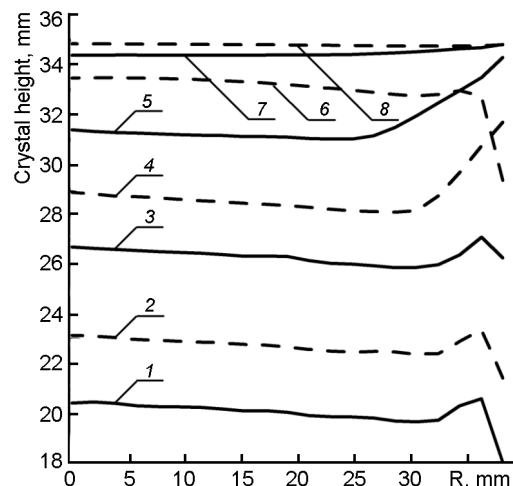


Fig. 4. Crystallization front position dependences on circular gap width in lateral insulation: 1, width 1 mm, diaphragm closed; 2, width 3 mm, diaphragm closed; 3, width 5 mm, diaphragm closed; 4, width 6 mm, diaphragm closed; 5, width 7 mm, diaphragm closed; 6, width 9 mm, diaphragm opened; 7, width 1 mm, diaphragm opened; 8, width 5 mm, diaphragm opened.

thermal fluxes at the crystallization front due to changes of radiation fluxes from opened lower crystal butt to the environment. The most substantial changes occur in circular areas corresponding to diaphragm areas being opened/closed. It is enough to change the diaphragm aperture within narrow limits for precise control of crystallization process. The diaphragm height position and thermal-physical properties of diaphragm and surrounding constructions have been considered. It is possible to control the crystallization front shape as well as to change the melt thickness within some limits by height change or screening of the gap in lateral heat-insulation against the melt opened area.

This work was supported partially by INTAS Project No.05-100008-8111.

### References

1. V.D.Golyshev, M.A.Gonik, V.B.Tsvetovskiy, *J. Cryst. Growth*, **198/199**, 501 (1999).
2. V.I.Goriletsky, B.V.Grinyov, B.G.Zaslavsky, *Crystal Growth*, Akta, Kharkiv (2002) [in Russian].
3. V.I.Deshko, A.Ya.Karvatsky, A.V.Lenkin, Y.V.Lohmanets, in: *Abstr. V-th Intern. Conf. on Problems of Industrial Heat Engineering*, May 22-26, 2007, Kyiv, Ukraine, p.83.
4. V.I.Deshko, A.Ya.Karvatsky, A.V.Lenkin, V.D.Golyshev, in: *Abstr. XII Russian Nation.*

- Conf. on Crystal Growth, Moscow, 23–27 October 2006, p.153 [in Russian].
5. V.I.Deshko, A.Ya.Karvatsky, A.V.Lenkin, in: Abstr. IV Intern. Conf. on Problems of Industrial Heat Engineering, Sept. 26–30, 2005, Kyiv, Ukraine, p.278.
  6. S.V.Bykova, V.D.Golyshev, M.A.Gonik et al., *J. Cryst. Growth*, **266**, 246 (2004).
  7. Boundary Element Methods in Heat Transfer, ed. by L.C.Wrobel, C.A.Brebbia, CMP Southampton Boston & Elsevier Applied Science, London & New York (1992).
  8. A.J.Karvatskii, *Naukovi Visti NTUU "KPI"*, No.1, 83 (1999).
  9. A.Ya.Karvatsky, P.I.Dudnikov, S.V.Leleka et al., in: *Materialy Miedzynarodowej Konferencji "Dynamika Naukowych Badan – 2007"*. Nauka i Studia, Przemysl (2007), v.9, p.33.
  10. V.I.Deshko, A.Ya.Karvatsky, A.V.Lenkin, *ENERGETIKA: Ekonomika, Tehnologii, Ekologiya*, No.1, 65 (2005).
  11. V.I.Deshko, A.Ya.Karvatsky, A.V.Lenkin, *Naukovi Visti NTUU "KPI"*, No.3, 20 (2003).

## **Розробка методів керування тепловими режимами для безтигельного методу ОТФ**

**В.І.Дешко, В.Д.Голишев, А.Я.Карвацький, Ю.В.Лохманець**

Розглядаються результати дослідження можливостей керування вирощуванням кристалів безтигельним методом ОТФ. Чисельні дослідження виконані на базі спеціально розробленої моделі глобального теплообміну. Розглянуто методи керування, що базуються на зміні радіаційних потоків. Встановлено, що при зміні ступеня відкритості діафрагми у діатермічній області під кристалом і зазору у бічній теплоізоляції навпроти розплаву істотно змінюються температурні поля й теплові потоки на фронті кристалізації внаслідок зміни радіаційних потоків у навколишнє середовище. Проведено аналіз впливу розташування діафрагми за висотою та теплофізичних характеристик діафрагми і навколишніх конструкцій на положення й форму фронту.